C·1

A TWO DIRECTIONAL STUDY OF SCATTERING OF RUBY LASER LIGHT FROM A PLASMA JET

by

LAWRENCE ALLAN GODFREY

B.Sc., University of British Columbia, 1971

A THESIS PRESENTED IN PARTIAL FULFILMENT OF

THE REQUIREMENTS FOR THE DEGREE OF

MASTER OF SCIENCE

in the Department

of

Physics

We accept this as conforming to the

required standard

THE UNIVERSITY OF BRITISH COLUMBIA

September, 1973

In presenting this thesis in partial fulfilment of the requirements for an advanced degree at the University of British Columbia, I agree that the Library shall make it freely available for reference and study. I further agree that permission for extensive copying of this thesis for scholarly purposes may be granted by the Head of my Department or by his representatives. It is understood that copying or publication of this thesis for financial gain shall not be allowed without my written permission.

Department of Physics

The University of British Columbia
Vancouver 8, Canada

Date September 1, 1973

ABSTRACT

A two channel system is used to study, simultaneously in two directions, the scattering of ruby laser light from a plasma jet. The experimental scattering spectrums compare well with theoretical predictions for scattering from an infinite homogeneous thermal plasma. The fluctuations in the integrated spectrums for the two directions are shown to be positively correlated, as well as to be too large to be accounted for by known sources of fluctuation. Changes in the plasma parameters, electron density and temperature, are ruled out as the source of the extra fluctuations.

TABLE OF CONTENTS

LIST OF FIGURES

ACKNOWLEDGEMENTS

I would like to thank Dr. R.A. Nodwell for his advice and encouragement during this experiment. My thanks also go to Dr. H. Baldis for his many helpful hints, to Mr. D. Sieburg and Mr. J. Aazam-Zanganeh for their technical assistance, and to Dr. M. Churchland, Mr. Gary Albach, and other members of the Plasma Physics Group for their discussions of this experiment.

Chapter I

INTRODUCTION

The experimental results for scattering of electromagnetic radiation from free electrons in a plasma have, in general, been in good agreement with theoretical predictions. However, there have been many examples of deviations from theoretical predictions, usually involving enhancements in the scattering spectrum in the region of the frequency shift corresponding to the plasma frequency, ω_p, or at multiples of 1/2 ω_p (Gerry and Rose,[1] Evans *et al.*,[2] Ringler and Nodwell,[3,4,5] Churchland[6]). Another possibility of anomalous scattering was noted by D. H. Baldis while scattering laser light from a plasma jet. The observed standard deviation of the scattered signal appeared to be too large to be accounted for by photon statistics and other known sources of fluctuations. It was suggested some non-thermal characteristic of the plasma could produce the extra observed flucuation.

This experiment was performed to investigate the fluctuations in scattering signal, to determine if

these fluctuations can be accounted for by known sources, and to try to determine another source of fluctuation if they cannot. For this purpose, a two channel system was adopted. This allowed not only the study of the scattered signal simultaneously in two directions, but also the study of the correlation of the two scattered signals. The shape of the scattered spectrum was carefully measured to determine the plasma parameters, electron density (N_e) and electron temperature (T_e). Then the integrated scattering spectrum was observed in order to measure the fluctuations in the scattered light for the two directions, as well as the correlation between the two signals.

Chapter II gives a brief summary of scattering theory for a homogeneous infinite plasma. A method, due to Kegal, of determining the electron density and temperature from scattering profiles is presented, as well as the theoretical dependence of the scattering signal on N_e and T_e.

Chapter III is devoted to a description of the experimental apparatus. Chapter IV describes the experimental method and results. A discussion of the results is also presented in Chapter IV. The conclusion is given in Chapter V, and a detailed description of the alignment procedure is presented in Appendix A.

Chapter II

THEORY

A. Summary of Scattering Theory

The theory of scattering of light from free electrons in a plasma has been derived by many authors (for example see Saltpeter,[7] Rosenbluth and Rostoker[8]), so only a brief summary is given here.

The theory is based on the classical approach; that is electromagnetic radiation incident on the plasma causes the free electrons to be accelerated, which in turn causes the electrons to radiate. The intensity of the scattered radiation from the electrons is equal to the ensemble average of the electric field vectors from a large number of electrons. The relative positions of the electrons will result in different phase shifts of the electric field vectors; their relative velocities, different frequency shifts.

Unless there is some spatial nonuniformity in the charge distribution, the resultant scattered signal

will be zero in all directions except parallel to the incident wave vector. This nonuniformity can arise from the particle nature of the plasma resulting in density fluctuations. The density fluctuations can be thought of as a combination of random thermal waves in the plasma. Thus the laser light is scattered from random thermal waves in the plasma, and their frequency and spatial distribution will determine the shape of the scattering spectrum. It is also possible to have spatial charge distribution nonuniformity due to macroscopic variations of electron density.

The differential scattering cross section for scattering through an angle θ is given by:

$$\sigma\left(\underline{k}-\underline{k}_o,\omega-\omega_o\right) = \frac{r_o^2}{2}\left(1-\sin^2\theta\cos^2\phi\right)\frac{1}{n_o}S\left(\underline{k}-\underline{k}_o,\omega-\omega_o\right)$$

where:

- r_o is the classical radius of the electron
- ϕ is the angle between the direction of polarization of the incident radiation and the scattering plane
- n_o is the average electron number density
- $\underline{k}_o$ is the incident wave vector
- $\underline{k}$ is the scattering wave vector

ω_o is the incident wave frequency

ω is the scattering wave frequency

$S\left(\underline{k}-\underline{k}_o, \omega-\omega_o\right)$ is the spectral density distribution.

See Fig. II-1 for the geometry of the laser light scattering.

The spectral density distribution is given by the Fourier transform of the autocorrelation function of the electron density:

$$S\left(\underline{k}-\underline{k}_o, \omega-\omega_o\right) = FT\left(C_n(\underline{\Delta}, \tau)\right)$$

$$C_n\left(\underline{\Delta}, \tau\right) \equiv \frac{1}{V_p} \int_{V_p} \underline{dr}\, \frac{1}{T} \int_{-T/2}^{T/2} dt\; n_e\left(\underline{r}, t\right)\; n_e\left(\underline{r}+\underline{\Delta}\,, t+\tau\right)$$

$$FT\left(f(\underline{r}, t)\right) \equiv \int \underline{dr}\; dt\; f\,(r,t)\; \exp\left[-\, i\left((\omega-\omega_o)t - (\underline{k}-\underline{k}_o)\cdot \underline{r}\right)\right]$$

For a Maxwellian plasma this gives:

$$S\left(\underline{k}-\underline{k}_o, \omega-\omega_o\right) = \frac{2\pi n_o}{|\underline{k}-\underline{k}_o|} \frac{F_e|1 - G_i|^2 + Z\, F_i|G_e|^2}{|1 - G_e - G_i|^2}$$

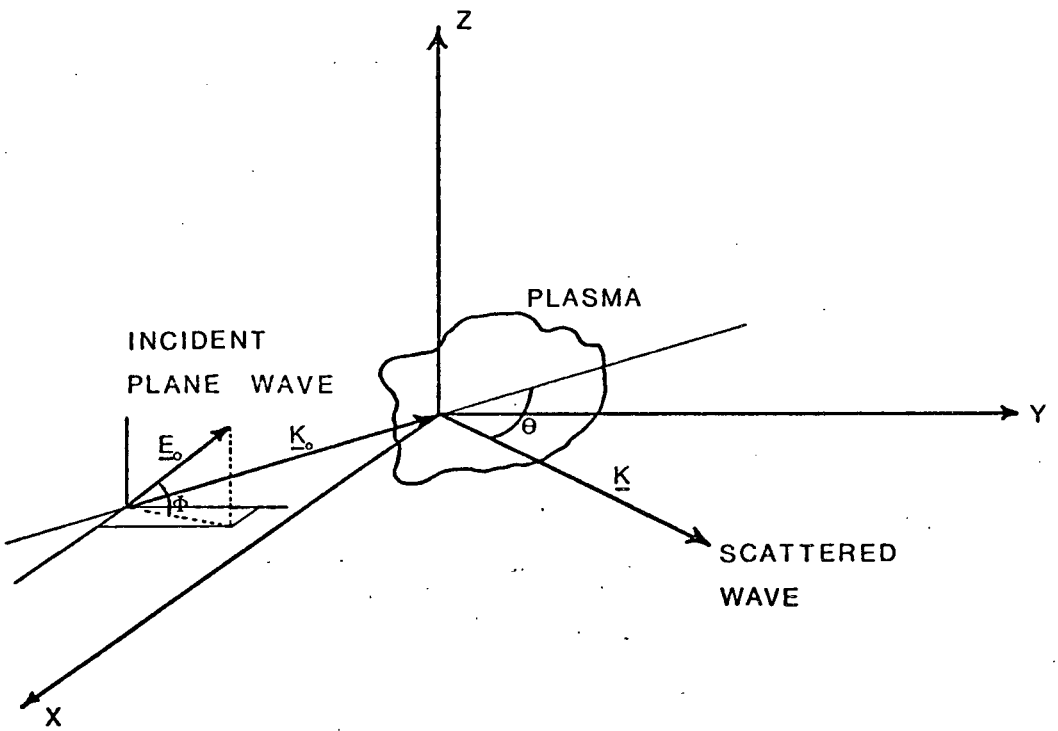

FIG II-1
SCATTERING OF PLANE ELECTROMAGNETIC RADIATION FROM A PLASMA

where: subscript e refers to the electrons

subscript i refers to the ions

T is temperature

m is the mass of the particle

κ is Boltzman's constant

$$F = (m/2\pi\kappa T)^{\frac{1}{2}} \exp(-X^2)$$

$$X_e = (m_e/2\kappa T_e)^{\frac{1}{2}}(\omega-\omega_o)/|\underline{k}-\underline{k}_o|$$

$$X_i = \left(\frac{m_i T_e}{m_e T_i}\right)^{\frac{1}{2}} X_e$$

$$G = -\alpha^2\left[1 - 2x\exp(-X^2)\int_0^x \exp(-t^2)dt + i\pi^{\frac{1}{2}} x \exp -X^2\right]$$

$$\alpha_e = \left(\frac{4\pi n_o e^2}{\kappa T_e}\right)/|\underline{k}|$$

$$\alpha_i = \left(\frac{Z T_e}{T_i}\right)^{\frac{1}{2}} \alpha_e$$

B. Determining Electron Density and Temperature from Experimental Scattering Profiles

In general, when $S(\underline{k}-\underline{k}_o,\omega-\omega_o)$ is plotted as a function of X_i or X_e, or preferably as a function of $\log_{10}(\Delta\lambda)$, $\Delta\lambda = \lambda-\lambda_o$, with α_e, N_e, T_e, and T_i as parameters,

there is an ion feature and an electron feature. The ion feature is very close to the central laser frequency and is usually difficult to investigate. The electron feature can be used to determine the electron density and temperature. The shape of the electron satelite, when normalised to its maximum and plotted as function of $\log(\Delta\lambda)$, is completely determined by the parameter α: changes in N_e and T_e that keep the same α merely serve to shift the spectrum along the $\log(\Delta\lambda)$ axis. Using this principle it is possible to determine N_e and T_e from the scattering spectrum in the following manner, due to Kegal.[9]

A standard set of theoretical graphs is drawn for different α of $S(\underline{k}-\underline{k}_o,\omega-\omega_o)/S_{max}$ versus $\log_{10}(\Delta\lambda)$, keeping T_e,T_i,θ,ϕ constant, with $T_i = T_e$, and changing N_e as required. Then the experimental graph of the scattered signal, normalised to the incident radiation and the maximum scattering signal, versus $\log_{10}(\Delta\lambda)$ is compared to the theoretical plots. Once the theoretical graph is found that has the same shape as the experimental graph (i.e. the experimental α is determined) the electron temperature and density can be calculated using the shift Δ. Δ is the amount that the theoretical graph must be moved along the $\log_{10}(\Delta\lambda)$ axis of the experimental graph so that the two graphs coincide. The electron density and temperature are then given by:

$$\log_{10}T_{ex} = \log_{10}T_{st} + \log_{10}\left[\sin^2(\theta_{st}/2)\right]$$

$$- \log_{10}\left[\sin^2(\theta_{ex}/2)\right] + 2\Delta$$

$$\log_{10} N_{e_{ex}} = \log_{10} N_{e_{st}} + 2\Delta$$

where the subscripts ex and st refer to the experimental and standard values respectively.

A slight change was made from Kegal's method to facilitate fitting actual experimental results. In the theoretical profiles, the maximum value is well defined. However, in experimental results the true maximum is seldom observed. This can result in incorrect normalisation of the experimental results. To counteract this, the vertical axis was changed to a $\log_{10}$ scale, which allows small up and down shifts when comparing the experimental and theoretical graphs.

C. Theoretical Calculation of Signal Dependence on Electron Density and Temperature

Since it is to be determined if the experimental fluctuations are too large to be accounted for by known sources of fluctuation, a calculation must be performed

to determine the changes in the two scattering signals if there are small changes in N_e and/or T_e. The mechanisms for shot-to-shot variation in N_e and T_e will be discussed in the last section of Chapter IV.

The total signal detected by the photomultiplier will be a convolution of the scattering spectrum and the transmission function of the monochromator. The instrument profile can be determined experimentally, and depends on the wavelength setting and the width of the entrance and exit slits. Let $T(\omega)$ be the transmission function on the monochromator for a given frequency setting and exit and entrance slits. The experimental signals are normalised to the incident radiation, and $\phi = 90°$, so we have

$$\frac{P_{Scat}\left[\underline{k}-\underline{k}_o, \omega-\omega_o\right]}{I_o} \alpha\ S(\underline{k}-\underline{k}_o, \omega-\omega_o)$$

where P_{Scat} is the scattered power, and I_o is the incident intensity. Since we are not interested in absolute values, constants may be neglected, and the signal at the photomultiplier is then given by:

$$S_{PM}\left(\theta_{Scat}\right) = \int_{-\infty}^{+\infty} T(\omega) S\left(\underline{k}-\underline{k}_o, \omega-\omega_o\right) d\omega$$

for the given monochromator settings.

This calculation was done for $N_e = 2.07 \times 10^{16}$ cm^{-3}, T_e = 19,000 °K, and scattering angles 49° 22' and 130° 32'. First N_e was varied by ±50% from the value quoted above, while T_e was kept constant. Then T_e was varied by ±50% while N_e was kept constant. Finally both N_e and T_e were varied in such a manner as to keep the same α. The monochromator had the transmission function shown in Fig. II-2, centred over the electron satellite peak for the forward direction. The wavelength setting was 6972 Å, the exit slit 2 mm wide and the entrance slit 400μ wide. Fig. II-3 shows the results of this calculation.

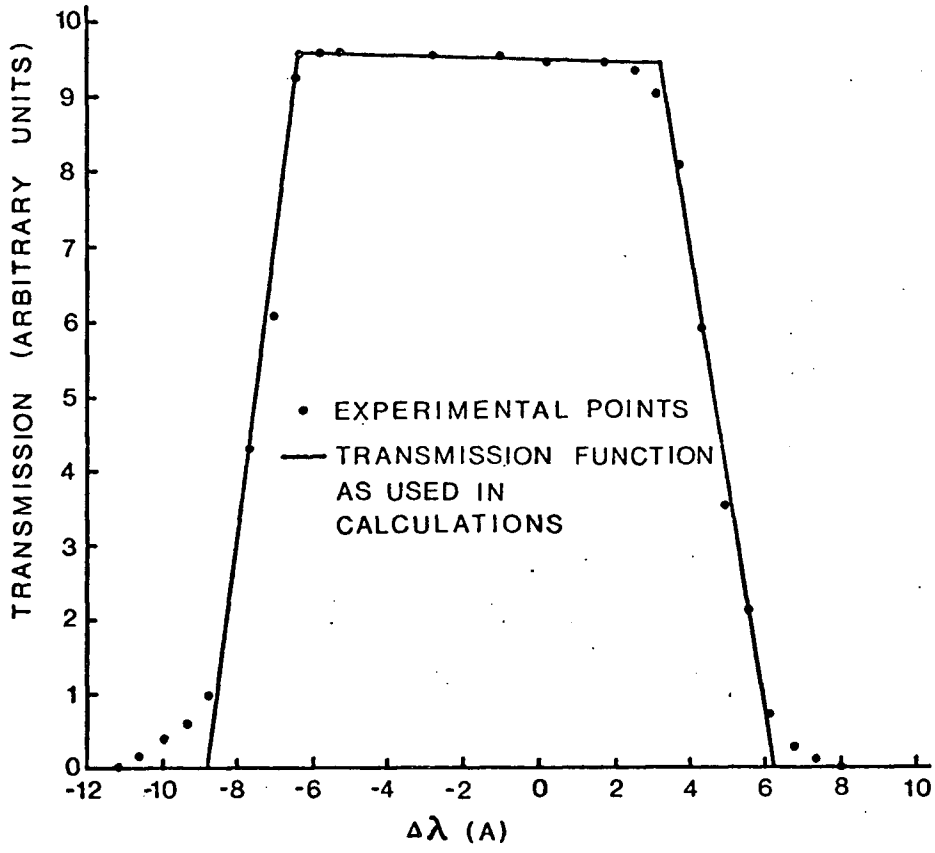

FIG II-2
MONOCHROMATOR TRANSMISSION FUNCTION - WIDE PASSBAND

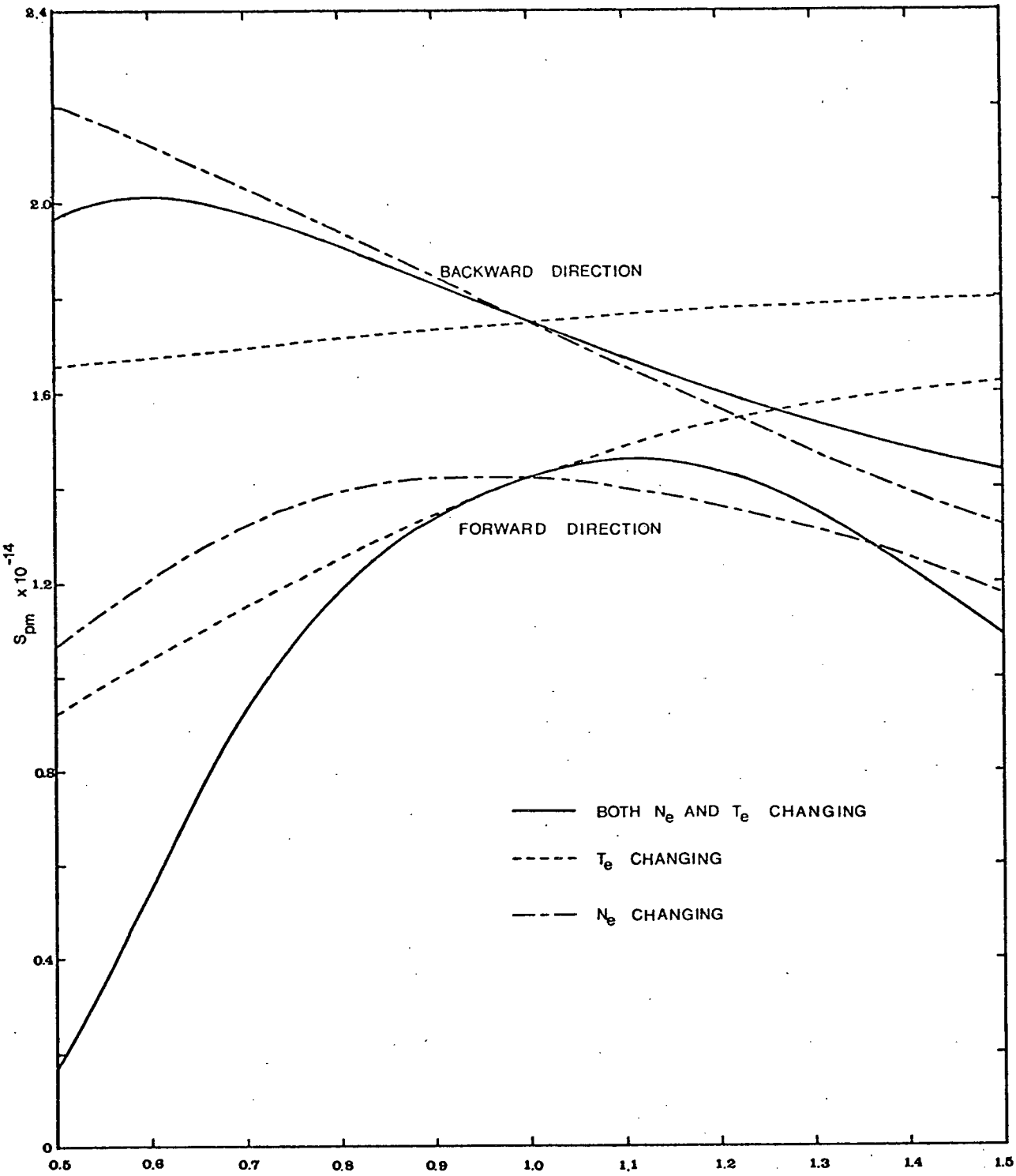

FIG II-3

THEORETICAL DEPENDENCE OF SCATTERED SIGNAL ON N_e AND/OR T_e CHANGING

Chapter III

EXPERIMENTAL APPARATUS

Fig. III-1 is an illustration of the experimental arrangement. Light from the ruby laser is focussed into the plasma jet. Scattered light is collected at 49° 28' and 130° 38' to the axis of the ruby laser and detected by a monochromator and photomultiplier.

A. The Plasma Jet

The plasma jet used in this experiment is similar to that used by Chan[10] and Baldis[11] (see Fig. III-2). For a complete description of the construction of a plasma jet see Morris.[12] The jet is run with helium rather than argon since helium has considerably less continuum radiation than argon. Also the helium jet is much less likely to be perturbed by the laser pulse (van der Kamp[13]).

The jet is idled at low current, about 70 amps, with a Miller model SRH 333s welding supply. When the laser is to be fired, the current source is changed to a

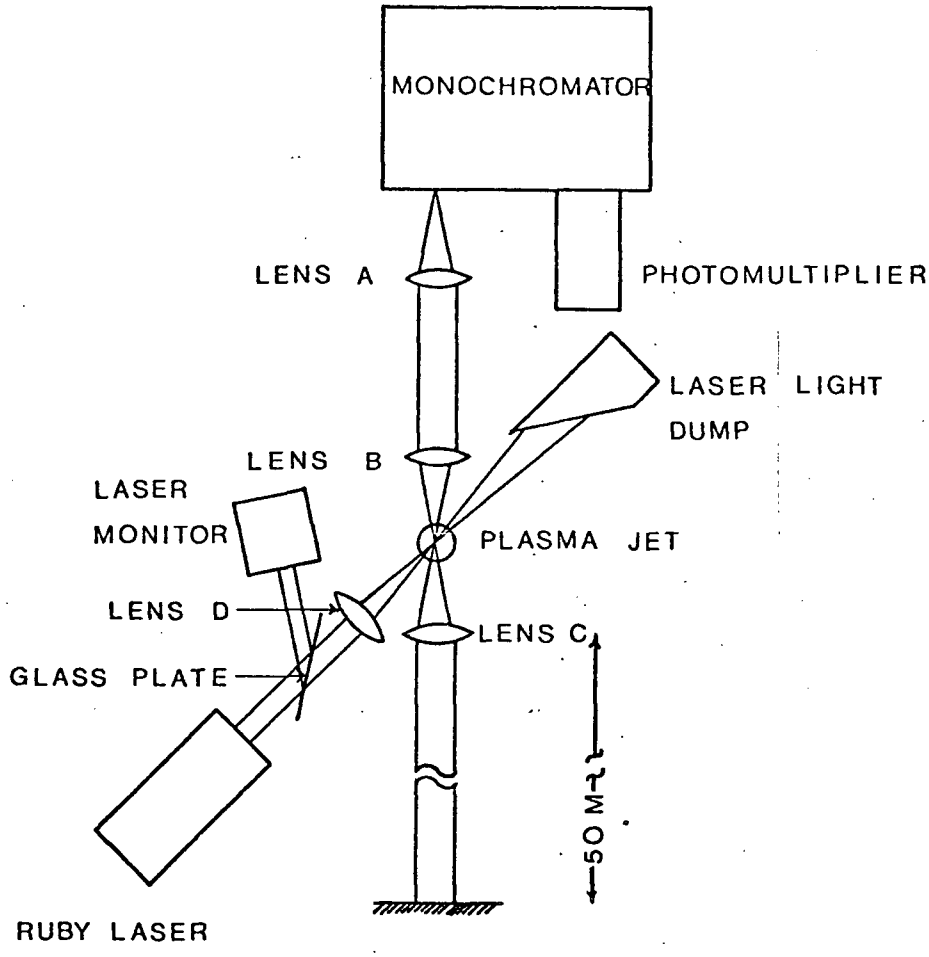

FIG III-1
EXPERIMENTAL ARRANGEMENT

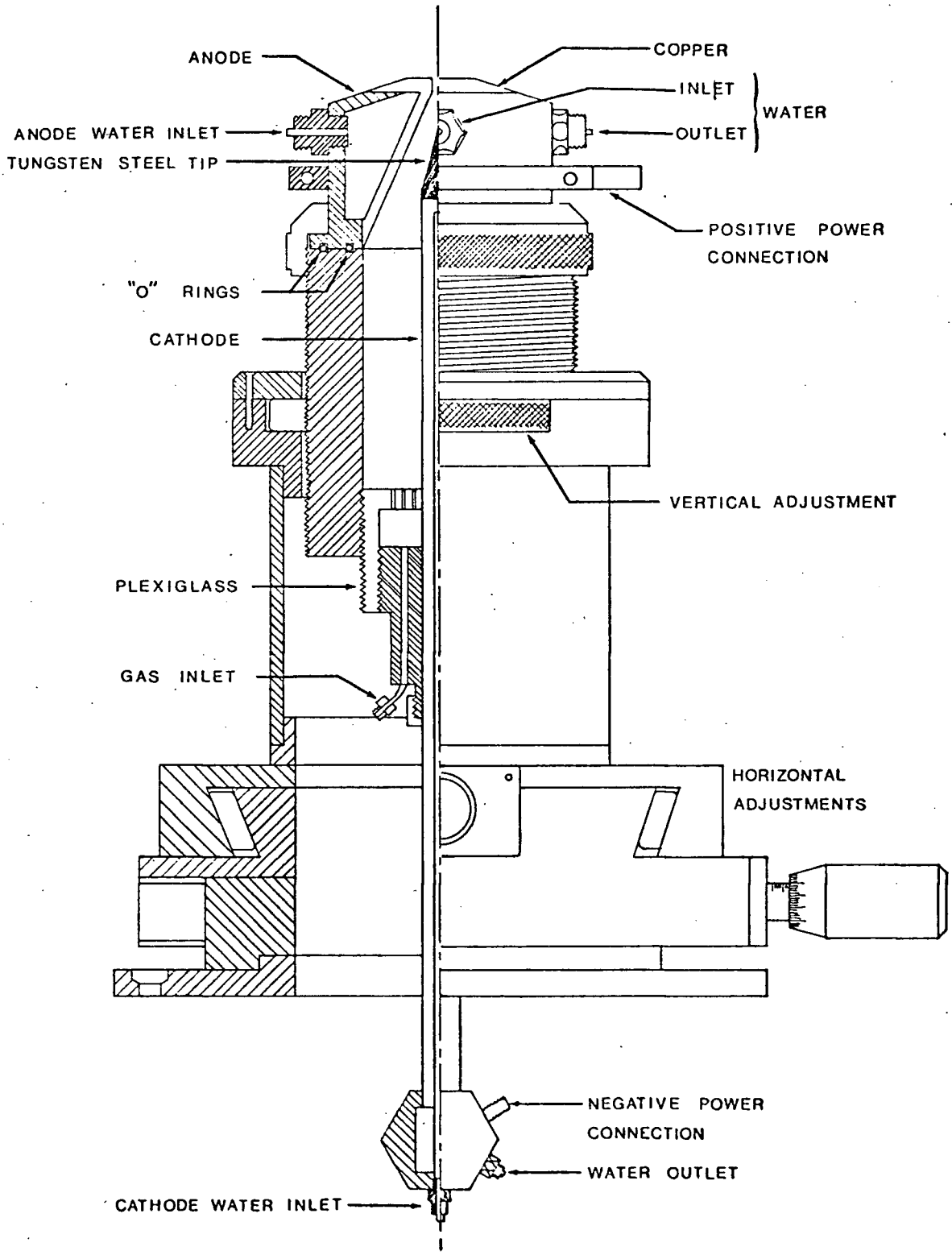

FIG III-2
SCHEMATIC OF THE PLASMA JET, ~ 3/4 SCALE
ALL MATERIAL BRASS, EXCEPT WHERE NOTED

48 volt, 240 amp-hour battery, and the current raised in six steps to 230 amps by paralleling combinations of one ohm, 1000 watt resistors with the ballast resistor (Fig. III-3). The large number of steps reduces the erosion of the water-cooled anode and cathode, thereby increasing the reproducibility of the jet. The current is then adjusted exactly to 230±3 amps using a current and voltage regulated power supply (Trygon Electronics Model M36-30a). The jet is allowed a few seconds to come to equilibrium, and then the laser is fired.

The jet current is monitored by measuring the voltage drop across a 10^{-4} ohm shunt with a digital voltmeter (Dana 3800) which reads to the nearest tenth of a millivolt. This gives a direct reading of the current: 1 mv = 10 amps. The shunt is accurate to 1% and the voltmeter to 0.1 mv., so that the current could be set to 230±3 Å., but could be set to the same current from shot-to-shot to within 1 amp.

The axis of the jet is vertical, and perpendicular to the monochromator and laser axis.

B. The Ruby Laser

A modified TRG Model 104 ruby laser is used in this experiment, capable of a 20 megawatt pulse with a 35

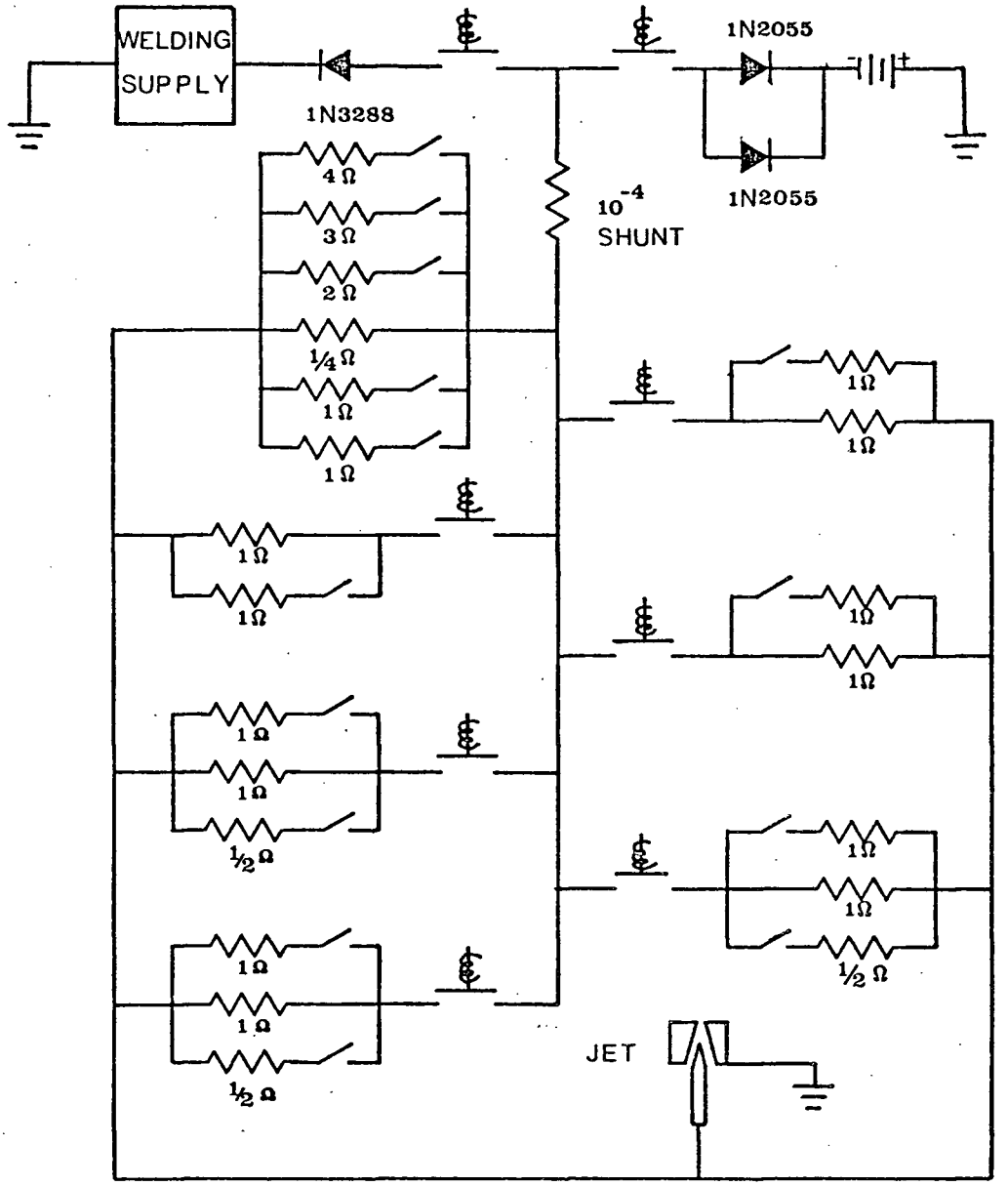

FIG III-3

PLASMA JET POWER SUPPLY CIRCUIT

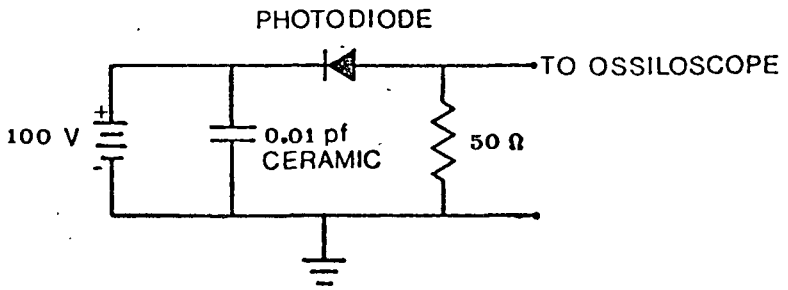

FIG III-4 LASER MONITOR CIRCUIT

nsec width at half intensity. The laser is Q-switched with a corner reflecting prism, rotation at 30,000 rpm. The front mirror of the laser cavity has 40% reflectivity at 6943 Å. The glass ruby rod holders have been modified slightly to accept a 3/8 inch diameter rod rather than the original 10 mm. diameter rod. The 3 inch long ruby rod and one flash tube are air cooled. The capacitor bank contains 1000 joules at about 900 volts.

The laser light is focussed into the plasma and then absorbed in a copper sulphate solution light dump with an entrance window at the Brewster angle. The electric vector of the laser light is perpendicular to the scattering plane ($\phi = 90°$).

The laser is monitored by reflecting some of the laser light from a thin glass plate, placed at the Brewster angle between the laser and the plasma, on to a solid state photodiode. The diode, a Hewlett-Packard part #5082-4220, is biased at 100 volts to give a fast risetime (less than 1 nsec), and linearity up to 10 volts. Sufficient neutral density filters are placed in front of the photodiode to keep it operating in its linear region (actual signals about 0.5 volts). Fig. III-4 shows the circuit for the laser monitor.

the detecting system is very critical, a detailed description of the alignment procedure is presented in Appendix A.

There are several obvious advantages of this optical delay system over a two monochromator, two photomultiplier system. First, of course, is the convenience of having only one monochromator and photomultiplier as well as the reduced expense. Also, there is no problem of calibrating the two monochromators so that they are analyzing the same wavelength, or have the same transmission function. There is no problem of different spectral sensitivities of two different photomultipliers. The disadvantages are the very critical alignment and the high loss in the delay section (35%). The 35% loss is not unreasonable considering 4% loss each time the scattered light enters or leaves lens C, and possible 10-20% loss on reflection from the alluminum coated mirror.

The grating monochromator, built in our laboratory, is used in 5th order with linear dispersion of about 4.5 Å/mm, and a theoretical resolving power of about 30,000. A Kodak filter #29 is used to isolate the orders. The collecting lenses are stopped to match the monochromator speed f/6. For a complete description of the monochromator see VanAndel.[14]

Two photomultipliers were used. A high gain tube, RCA 7265, was mainly used which had a S-20 response

and nominal quantum efficiency of 3% at 6943 Å. A RCA 31034 was also used, which had an extended response in the red due to its GaAs photocathode surface. Its quantum efficiency of 16% should give an improvement in signal to noise of about a factor of 3 over a photomultiplier with a S-20 response. The RCA 7265 was operated at 2200 volts, and the RCA 31034 at 1900 volts.

A dual beam oscilloscope, Tektronix 551, with type L plug in units is used to record the signals from the photomultiplier and laser monitor. The traces are recorded on Polaroid type 410 film. The combined rise-time of the oscilloscope and plug in units is about 15 nsec, wich serves to integrate the signal slightly and improve the signal to noise.

To help to reduce the stray light, the detection system from lens B to the monochromator is encased in a light proof tube, and the laser is covered except for an exit hole for the laser light.

Chapter IV

EXPERIMENTAL RESULTS AND DISCUSSION

The purpose of this chapter is to present and discuss the experimental results. First, the scattering profiles and the determination of the electron density and temperature are given. Then the results for the correlation and standard deviation of the forward and backward scattering signals are presented. An estimate of the fluctuations due to different sources is made and then the results are discussed.

For all the experimental work, the following conditions apply. The jet was positioned so that the focal volume was centred 14.8 mm above the tip of the cathode, 1.8 mm above the anode. Also the scattering angles were 49° 22' in the forward directions, 130° 38' in the backward direction. The jet current was 230 amps and the helium flow rate was 32 cubic feet per hour. Except where noted, the RCA 7265 photomultiplier was used.

A. Scattering Profiles and Determination of N_e and T_e

So that work could be done with a plasma of known parameters, the scattering profiles and electron density and temperature were determined. For this purpose, the monochromator exit slit was set to 400μ wide to match the entrance slit, resulting in a triangular instrument profile, 1.8 Å half-width, as illustrated in Fig. IV-1. A run consisted of scanning the spectrum at least four times, with one scan composed of a shot every 1.8 Å from about 6955 Å to 7000 Å.

The oscillograms were then analyzed in a manner such that the electron density and temperature could be obtained as described in Chapter II. Fig. IV-2a shows a typical oscillogram. The maximum heights of the scattered signals were measured and normalised to the height of the laser monitor signal. The measurements for each wavelength were then averaged and standard deviations about the mean claculated. The means were then normalized to the maximum average signal, and a graph of the $\log_{10}$ of this normalised signal versus $\log_{10}(\Delta\lambda)$ was made. This experimental plot was then compared to a set of theoretical graphs for T_e = 16,000 °K, θ_{st} = 135°, α = 0.8 to 1.2 and 1.8 to 2.2 in steps of 0.05, so that α, N_e, T_e could be determined as described in Section II B.

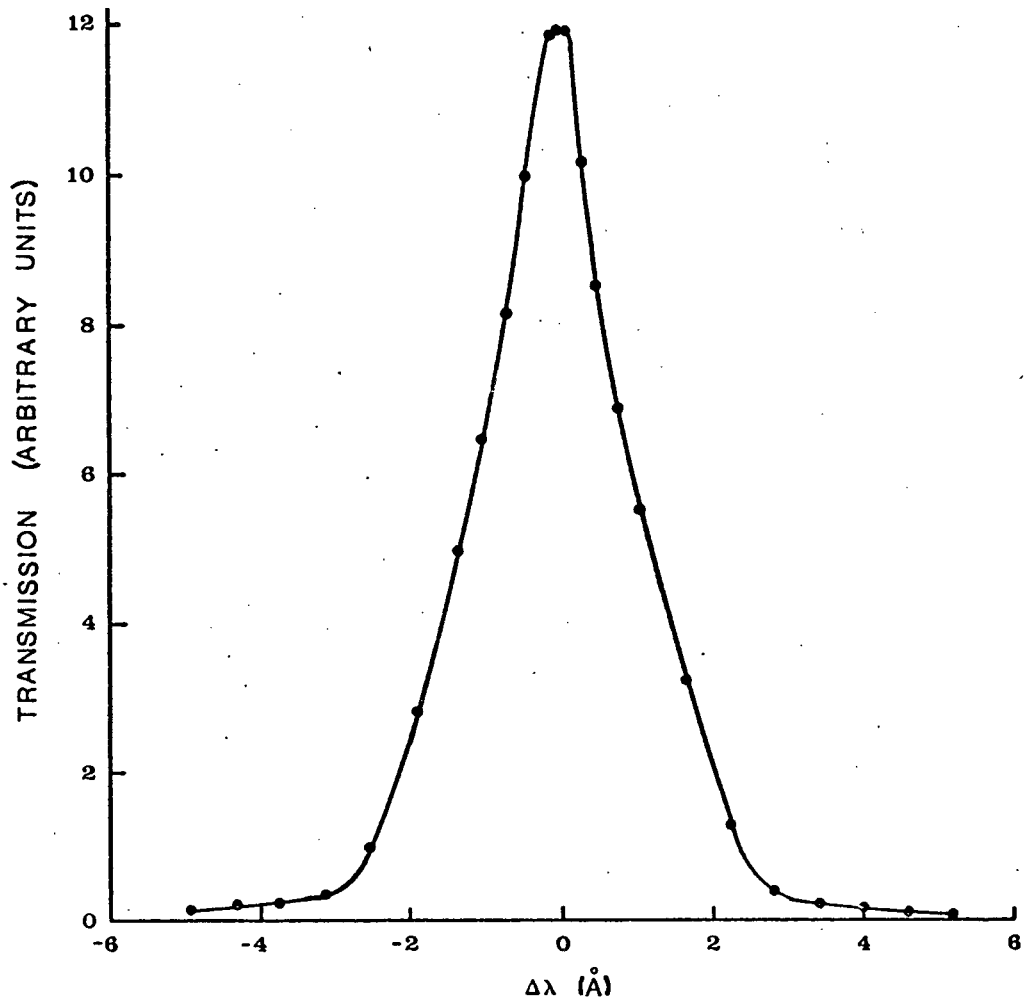

FIG IV-1

MONOCHROMATOR TRANSMISSION FUNCTION – NARROW PASSBAND

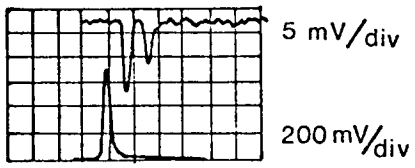

a. NARROW EXIT SLIT
RCA 7265 PM TUBE

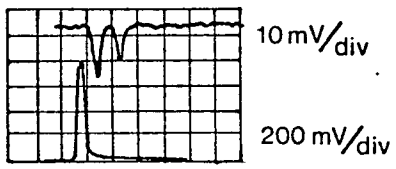

b. WIDE EXIT SLIT
RCA 7265 PM TUBE

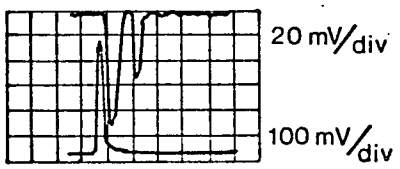

c. WIDE EXIT SLIT
RCA 31034 PM TUBE

FIG IV-2
TYPICAL OSCILLOGRAMS
$\lambda = 6972$; 100 nsec/div

For scattering in the forward direction, α was found to be 2.0. The electron density and temperature were:

$$T_e = 19{,}000\ ^\circ K$$

$$N_e = 2.07 \times 10^{16}\ cm^{-3}$$

The sources of error for determining the plasma parameters in this fashion are the uncertainty in determining α and in determining the shift Δ. An estimate was made of the error by measuring the shifts for α obviously too large and too small (2.05 and 1.95 respectively) and calculating the electron temperature and density from these shifts. This gave the average deviations:

$$N_e = (2.07 \pm 0.13) \times 10^{16}\ cm^{-3}$$

$$T_e = (19{,}000 \pm 200)\ ^\circ K.$$

The scattering profile for the backward direction has a broad, Gaussian-like shape, characteristic of $\alpha \lesssim 1$. For low α, a wide range of α's give acceptable fits to the experimental results, so that it is difficult to obtain accurate values for α, N_e, T_e from the scattering profiles. The results obtained are:

$$\alpha = 0.95 \pm 0.15$$

$$T_e = 15{,}700 \pm 3{,}500\ ^\circ K$$

$$N_e = 2.0 \pm 0.4 \times 10^{16}\ cm^{-3}.$$

The errors quoted above, determined in the same manner as for the forward direction, reflect the insensitivity of the spectrum to N_e and T_e. However the values for electron density and temperature for the two directions and self-consistent.

Fig. IV-3 and Fig. IV-4 show the experimental results for the scattering spectrums, along with the theoretical graphs of $S(\underline{k}-\underline{k}_o,\omega-\omega_o)/S_{max}$ using N_e and T_e as determined from the scattering profile for the forward direction.

It should be noted that the scattering angles, geometrically measured using the entrance aperture at the monochromator, the hole in the jet anode, and the middle of the front mirror of the laser cavity as reference points, were 46° 25' and 133° 35'. However the presence of the focussing lens D can change the incident angle of the laser beam. The angles are difficult to measure with lens D affecting the incident radiation, so that the angle was determined to be that angle that gave good theoretical fits to the experimental data for both forward and backward scattering profiles. These angles, 49° 22' and 130° 38', when used for other experimental runs, also gave good theoretical fits to the two profiles, indicating that these were the proper scattering angles.

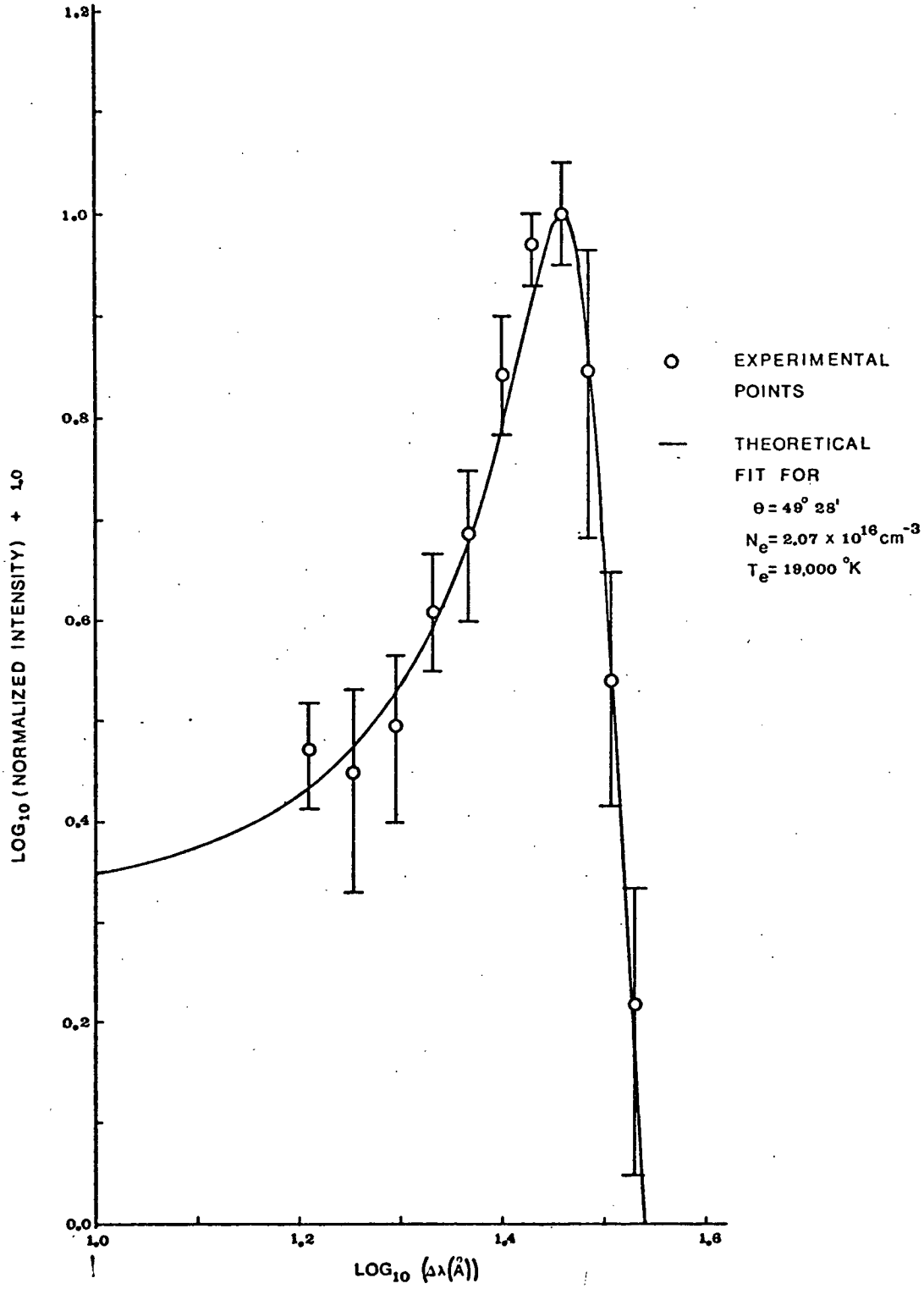

FIG IV-3
THEORETICAL FIT TO EXPERIMENTAL DATA FOR FORWARD SCATTERING

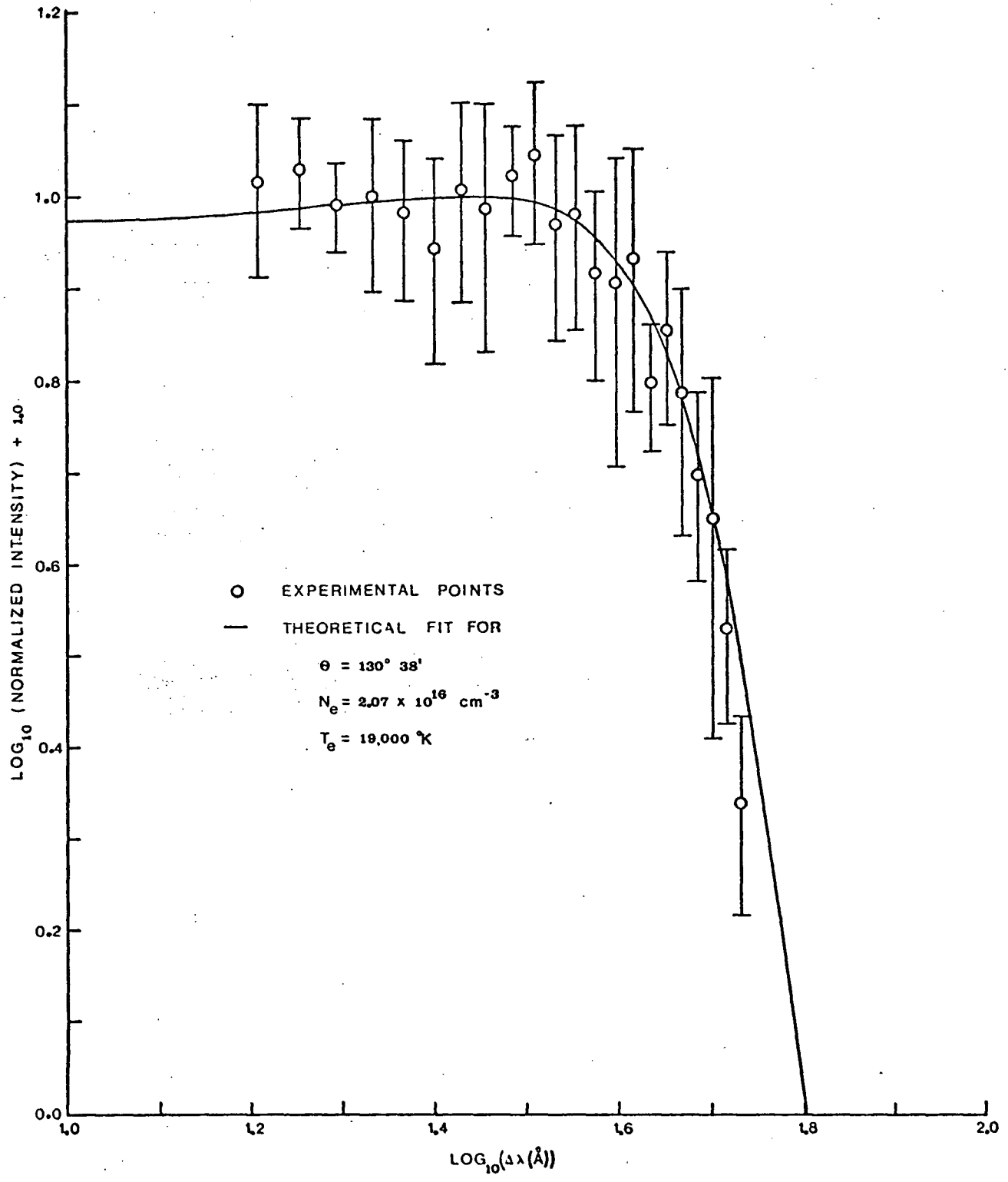

FIG IV-4
THEORETICAL FIT TO EXPERIMENTAL DATA FOR BACKWARD SCATTERING

B. Experimental Correlation and Standard Deviation

Once the plasma parameters were determined, the correlation between the backward and forward signals was studied, as well as the standard deviation of the two signals.

For this purpose, the monochromator exit slit was widened to 2.0 mm. This resulted in an instrument profile shown in Fig. II-2. The larger slit increased the total number of photons incident on the photomultiplier, and therefore reduced the shot noise. The monochromator was set so that the transmission function was centred on the electron satellite found in the forward scattering spectrum. Because of the 10 Å wide instrument profile, essentially all of the satellite was observed.

A series of at least 20 shots were fired, with a one-minute wait between shots. The one minute was necessary for the cooling of the laser, as well as making the power output more stable. Fig. IV-2b shows a typical oscillogram.

The height of the maximum of the forward and backward signals were measured and normalised to the height of the laser monitor signal. The means and standard deviations were then calculated. The coefficient of correlation between two variables X and Y is defined as:

$$\rho = \frac{\sum_i (\overline{X}-X_i)(\overline{Y}-Y_i)}{[\sum_i (\overline{X}-X_i)^2(\overline{Y}-Y_i)^2]^{\frac{1}{2}}}$$

where $\overline{X}$ means the average value of X, and X_i is the ith measurement of X. Because only the quantities $(\overline{X}-X_i)$ are used, it is unnecessary to subtract the stray light, approximately constant, from the observed signals. The presence of stray light will, however, contribute to the standard deviations of the signals. The contribution to the photomultiplier signal made by the stray light was corrected for when calculating the mean scattering signal.

A typical experimental result gave a coefficient of correlation of +0.85 for 25 shots. If the two signals were not correlated, there would be less than 1/2% chance of getting a coefficient of correlation equal to or larger than this. For all the runs, the coefficient of correlation was positive, with less than 10% chance of obtaining ρ equal to or larger than that observed. The standard deviations of the forward and backward signals were usually about 12-16% and 16-20% respectively.

Great care was taken to make the plasma conditions the same from shot-to-shot. The helium flow rate was set at the beginning of a run and never changed.

The current was reset to the same value to within less than 1/2%.

Two methods were used to operate the jet during a run. The jet was usually idled at about 70 amps as before, and then the current raised to 230 amps. However runs were also made with the current maintained at 230 amps. Both methods produced the large positive ρ.

The RCA 31034 photomultiplier was also tried. Fig. IV-2c shows the improvement in signal to noise, but the standard deviations of the signals actually were only reduced by one or two per cent. This is because there are other large sources of error which override the improvement in S/N. The coefficient of correlation remained at its high positive value.

C. Estimation of Known Fluctuations

To see if the scattering signals as measured in Section IV B. have more fluctuations than can be expected, estimates of the size of fluctuations from different sources were made. The sources considered were: shot noise due to the small number of photoelectrons, fluctuations due to the continuum radiation, fluctuations due to variations in stray light, and error in measurement of the signal heights.

To estimate the shot noise, the total number of photoelectrons had to be determined. The area under the curve of a signal from the photomultiplier is n times the area attributed to one photoelectron, where n is the total number of photoelectrons emitted from the photocathode surface. Thus if the size of the signal of one photoelectron can be determined, then the total number of photoelectrons can be estimated.

There are two main difficulties in determining the signal from one photoelectron. First, the signal is very small, less than 5 mv in height at the photomultiplier voltage used. Secondly, it is difficult to know whether or not the signal observed is due to a single photoelectron, to more than one, or due to an electron emitted from one of the dynodes. Inspite of these difficulties it was felt that this method was the most direct way of getting a good estimate of the number of photoelectrons. The manufacturer's specifications for the gain of the photomultiplier tube cannot be used for a good estimate, since there are such large variations in gain from tube to tube.

The signal from one photoelectron was determined in the following manner. The monochromator was set to 100 Å from the ruby laser wavelength so that the probability of more than one photon being detected by the photomultiplier

was small. When the laser was fired, the photomultiplier signal was usually flat, but occasionally there appeared a small signal. The position of the signal along the time axis varied, but the area of the signal remained constant. The triangular pulse was approximately 20 nsec wide at its base, and 2 mv high. Using this area it was then possible to estimate the number of photoelectrons in any photomultiplier signal as stated above.

For the case of a 10 Å bandpass situated on the electron satellite as described in Section IV B, it was estimated that there were 400 photoelectrons in the forward direction signal, and 300 in the backward. This would give a contribution of 5% and 6% to the standard deviations of the two signals respectively.

The existence of continuum radiation causes fluctuations in the baseline of the signal from the photomultiplier, and therefore contributed to the fluctuations in the scattering signals. An estimation of this contribution was made by considering that part of an oscillogram which has no scattering signal. Fifteen measurements were taken, one every 20 nsec over a 300 nsec range, of the position of the baseline from a horizontal graticule line. The standard deviation of this measurement was then compared to the average height

of the scattering signals. The standard deviations of the baseline was found to be about 5% and 8% of the forward and backward scattering signals respectively.

The stray light was assumed to originate from the laser light at 6943 Å entering the monochromator. Thus the stray light was proportional to the incident radiation. After the stray light signal was normalised to the laser monitor signal, it had a standard deviation of about 20%. Since the forward and backward signals were comprised of about 3% and 5% stray light, the stray light would contribute about 1/2% and 1% to the standard deviations of the forward and backward scattering signals.

The heights of the signals on the oscillograms were measured using a x10 magnifying glass with an estimated error of 2%.

The total estimated standard deviation of the scattering signals, adding the square of the individual estimates and taking the square-root, are 8% and 11% for the forward and backward scattering signals respectively.

D. Discussion

The scattering profiles are in excellent agreement with theoretical profiles for T_e = 19,000 °K,

$N_e = 2.07 \times 10^{16}$ cm^{-3}, and $\theta = 49° 22', 130° 38'$. The temperature is slightly higher than reported previously, (van der Kamp,[13] Chan,[10] Stansfield,[15] Baldis,[11] Morris[12]), but is within error of the values quoted by van der Kamp and Morris. The electron density is comparable to that reported earlier.

The total estimated standard deviation of the two scattering signals are both less than 3/4 of the actual standard deviations. The estimates are very rough, and the total deviation could be 2 or 3% low, but they are still much less than the observed deviations.

It was found that the fluctuations in the two scattering signals are highly correlated. If the fluctuations originated from shot noise, continuum radiation, and stray light alone, one would expect the fluctuations to be independent. The fact that the fluctuations are too large and are correlated indicates that there must be at least one other source of fluctuation, about 12% in magnitude and positively correlated for the two directions.

One might propose that if the electron density and/or temperature changed from shot-to-shot, then this might produce the required variation in signal.

Mechanisms that might change N_e and T_e are variations in the jet current or gas flow rate, or perhaps changes in position of the plasma jet flame due to erosion of the cathod or anode. The later would tend to increase or decrease both N_e and T_e at the same time. A shift of more than 1 mm off the centre of the jet would seem unreasonable: this would produce a change in N_e and T_e of 17% (Morris[12]). However, calculations of Section II-C show that if both N_e and T_e decrease by 20% then the signal in the forward direction should increase by 1½%, and in the backward direction, should decrease by 8½%. These changes are too small as well as having negative correlation rather than positive.

It is not obvious exactly the changes in N_e and T_e resulting from changes in the gas flow rate or jet current. However, if it is assumed that these or any other mechanism that changes the plasma parameters leaves one of T_e or N_e constant and changes the other, then this cannot provide the extra fluctuations as illustrated in Fig. IV-5 and IV-6. Fig. IV-5 is a theoretical graph of the signal as function of N_e assuming T_e constant at the experimental value of 19,000 °K, reproduced from Section II C. The experimental points plotted on this graph were determined in the following

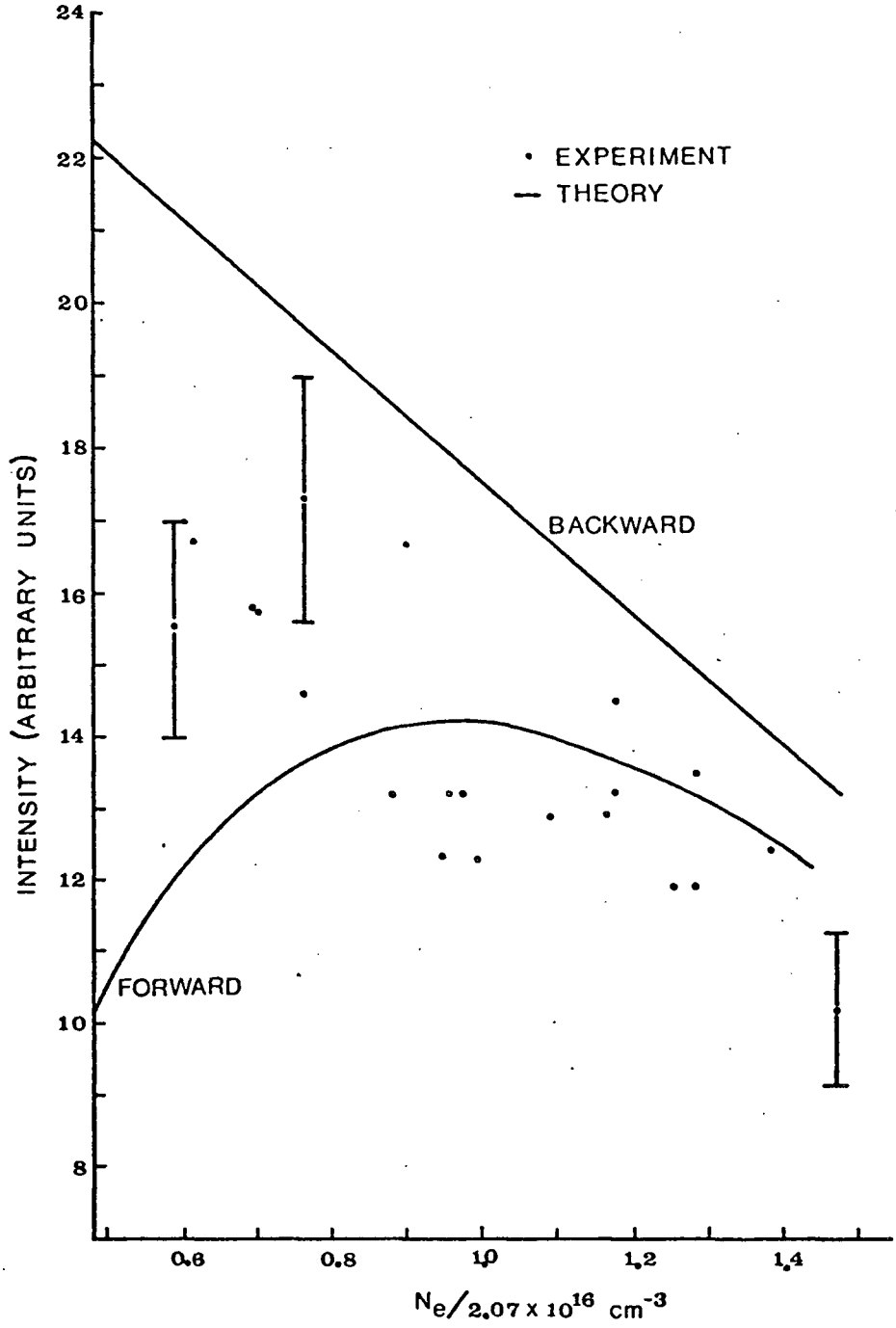

FIG IV-5
COMPARISON OF EXPERIMENTAL VARIATIONS IN SCATTERING SIGNAL TO CALCULATED VARIATIONS DUE TO CHANGING N_e

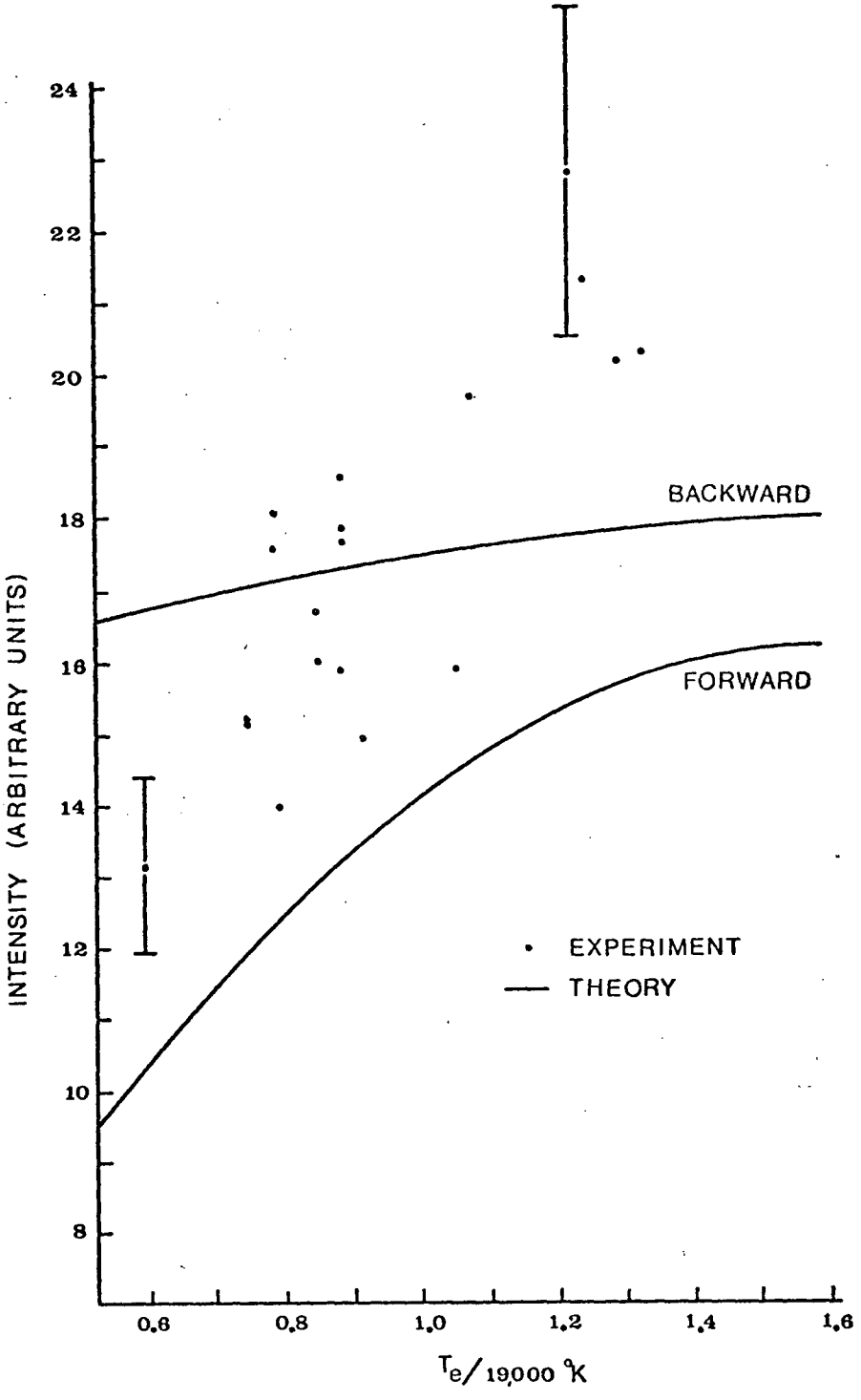

FIG IV-6
COMPARISON OF EXPERIMENTAL VARIATIONS IN SCATTERING SIGNALS TO CALCULATED VARIATIONS DUE TO CHANGING T_e

manner. Assume that an increase in the signal in the backward direction from its average value as measured in Section III B is due entirely to a change in N_e. This new N_e can be read from the graph IV-5. Using this new N_e, the new theoretical signal in the forward direction can be determined. The actual experimental forward signal is plotted at the new N_e, normalised so that the average forward signal is equal to the theoretical signal for T_e = 19,000 °K, N_e = 2.07 x 10^{16} cm^{-3}. If the changes in signal are really due to changes in N_e, then the experimental points plotted as described should lie about the theoretical curve for the forward direction. As can be seen from the graph, this is not the case. The error bars drawn come from the estimate made in Section IV C for all known sources of error.

A similar procedure was used to check if the variations are due to changes in T_e alone. This time the signal in the forward direction was used to find the new T_e and then the experiment points were drawn for the backward direction (Fig. IV-6). Again the theoretical curve and experimental points do not match up.

The above calculations indicate that the extra deviation is probably not due to fluctuations in N_e and T_e. It might still be possible for N_e and T_e to be

changing in some specific way to give the required deviations, but this does not seem reasonable because the variations in the calculated signal are too small unless very large changes (about 50%) are made in N_e and T_e. It would seem then that the plasma jet has some non-thermal characteristics which contribute to the standard deviation of the scattering signal, but are not so big as to cause large deviations from normal thermal scattering profiles.

Chapter V

CONCLUSIONS

A. Conclusions

Scattering profiles for scattering of ruby laser light from a plasma jet were measured simultaneously in two directions using a two channel system with optical delay. The experimental data agrees very well with theoretical profiles for scattering from and infinite homogeneous thermal plasma with $N_e = 2.07 \times 10^{16}$ cm^{-3}, $T_e = 19{,}000$ °K. The integrated scattering signal, measured with 10 Å wide monochromator trasmission function, proved to have a standard deviation too large to be accounted for by known sources of fluctuations. Also the integrated scattering signals for the forward and backward scattering angles had a large positive coefficient of correlation. Theoretical calculations show that the extra, correlated fluctuations cannot originate from changes in N_e and T_e. Thus it is suggested that the plasma jet has non-thermal properties that have only a

small effect on normal thermal scattering of laser light from a plasma jet.

B. Suggestions for Further Study

The dependence of the extra fluctuations and positive correlation on the scattering vector $\underline{k}$ could be studied. It may be possible for the non-thermal effects to have a sharp dependence on $\underline{k}$ such as Ringler and Nodwell found for the total integrated intensity of laser light scattered from a magnetically stabilised, low pressure hydrogen arc where the total integrated intensity was found to be approximately twice the theoretical value at one particular $\underline{k}$ vector, then dropped quickly to that predicted by theory as $\underline{k}$ was varied.

A multichannel system might be adopted where the entire scattering spectrum can be found with one firing of the laser. This would allow N_e and T_e to be determined from shot to shot, and therefore make the experiment more independent from changes in experimental parameters. Such a multichannel system is only recently on the market.

BIBLIOGRAPHY

1. Gerry, E.T. and Rose, D.J. 1966. J. Appl. Phys. 37: 2715-2724.

2. Evans, D.E. *et al.* 1966. Nature 211: 23-24.

3. Ringler, H. and Nodwell, R.A. 1969. Phys. Lett. 29A: 151.

4. Ringler, H. and Nodwell, R.A. 1969. Phys. Lett. 30A: 126.

5. Ringler, H. and Nodwell, R.A. 1969. Third Europ. Conf. on Contr. Fusion and Plasma Physics, Utrecht.

6. Churchland, M.T. 1972. Ph.D. Thesis, University of British Columbia.

7. Saltpeter, E.E. 1960. Phys. Rev. 120: 1528-1535.

8. Rosenbluth, M.N. and Rostoker, N. 1962. Phys. Fluids 5: 776.

9. Kegal, W.H. 1965. Internal Report. Institut fur Plasma Physik, IPP 6/34.

10. Chan, P.W. 1966. Ph.D. Thesis, University of British Columbia.

11. Baldis. H.A. 1971. Ph.D. Thesis, University of British Columbia.

12. Morris. R.N. 1968. Ph.D. Thesis, University of British Columbia.

13. van der Kamp, G.S.J.P. 1968. M.Sc. Thesis, University of British Columbia.

14. VanAndel, H.W.H. 1966. Ph.D. Thesis, University of British Columbia.

15. Stansfield, B.L. 1971. Ph.D. Thesis, University of British Columbia.

Appendix A

ALIGNMENT PROCEDURE

Because the alignment of the detecting system is critical, a detailed procedure is given here.

First a HeNe laser is aligned with the optical axis of the monochromator, the beam going in the exit slit which has been set to the required width. Then, with the monochromator set to transmit the laser line, two straight edges are placed 500μ apart over the 400μ wide entrance slit so that the rectangle formed is centred over the laser beam. This helps to define the volume of the observed plasma.

Next a front surface mirror is placed 50 meters away so that the laser beam hits approximately in the centre. The beam forms a diverging diffraction pattern when it leaves the monochromator, so it is 4 to 5 cm. wide at the mirror. Because of this, a stop was placed just in front of the mirror that has a series of concentric circles drawn on its face, centred around a 1/8

inch diameter hole. This stop is placed so that the hole is in the centre of the diffraction pattern, using the circles as a guide. The result is a small circle of light with some diffraction rings being reflected from the mirror. The mirror is then adjusted so that the reflected circle is centred on the entrance rectangle of the monochromator.

The lenses are now placed in their proper position along the axis of the detecting system with the aid of a telescope focussed to infinity. The telescope is placed between the mirror and the expected position of lens C centred on the laser beam. Lens A is approximately centred on the laser beam and then adjusted so that the image of the entrance slit is in the same plane as the cross hairs of the telescope. Thus the entrance slit-lens distance is equal to the focal length of lens A.

Next lens B and C are positioned. Lens B is placed so that it is about one focal length from the position of the plasma jet. The placement is not too critical because of the adjustments on the jet. Using the telescope again, lens C is placed so that the focal points of B and C coincide, which occurs when the image of the entrance slit is again in the same

plane as the cross hairs. Stops are placed on the optical benches so that the lenses can be removed and replaced without changing their position along the axis of the detection system.

Next is the adjustment of the horizontal and vertical positions of the lenses. Because of the greatly diverging beam after passing through a lens, there is no good reference for positioning lenses B and C by themselves. Together, however, there is a good reference beam since the only effect they have is to enlarge the beam by the ratio of their focal lengths. They are then aligned, with lens A removed, so that the laser beam is centred on both the aperture at the mirror and at the monochromator. Lastly lens A is positioned so that the beam is centred on the stop at the mirror, with both B and C in place.

The last step is to stop down the lenses so that they match the monochromator speed f/6. With the stop at the mirror removed, and f/3 lenses, focal lengths 12, 12, 30 cm. for A, B, and C respectively, the reflected laser beam should cover all the area of the lenses and be centred on each.

Because of the distance required, the first attempt at this experiment used three mirrors and five

reflections in the optical delay section to fold the light path. However, the extreme losses of this arrangement made it impractical, so that it was necessary to adopt a one mirror system.